1/f noise measurements for faster evaluation of electromigration in advanced microelectronics interconnections

Sofie Beyne, Kristof Croes, Ingrid De Wolf, and Zsolt Tőkei

Citation: Journal of Applied Physics **119**, 184302 (2016);
View online: https://doi.org/10.1063/1.4947582
View Table of Contents: http://aip.scitation.org/toc/jap/119/18
Published by the American Institute of Physics

JOURNAL OF APPLIED PHYSICS **119**, 184302 (2016)

1/f noise measurements for faster evaluation of electromigration in advanced microelectronics interconnections

Sofie Beyne,[1,2,a)] Kristof Croes,[2] Ingrid De Wolf,[1,2] and Zsolt Tőkei[2]
[1]*MTM, KU Leuven, Kasteelpark Arenberg 44 bus 2450, B-3001 Leuven, Belgium*
[2]*imec, Kapeldreef 75, B-3001 Leuven, Belgium*

(Received 24 December 2015; accepted 13 April 2016; published online 9 May 2016)

The use of 1/f noise measurements is explored for the purpose of finding faster techniques for electromigration (EM) characterization in advanced microelectronic interconnects, which also enable a better understanding of its underlying physical mechanisms. Three different applications of 1/f noise for EM characterization are explored. First, whether 1/f noise measurements during EM stress can serve as an early indicator of EM damage. Second, whether the current dependence of the noise power spectral density (PSD) can be used for a qualitative comparison of the defect concentration of different interconnects and consequently also their EM lifetime t50. Third, whether the activation energies obtained from the temperature dependence of the 1/f noise PSD correspond to the activation energies found by means of classic EM tests. In this paper, the 1/f noise technique has been used to assess and compare the EM properties of various advanced integration schemes and different materials, as they are being explored by the industry to enable advanced interconnect scaling. More concrete, different types of copper interconnects and one type of tungsten interconnect are compared. The 1/f noise measurements confirm the excellent electromigration properties of tungsten and demonstrate a dependence of the EM failure mechanism on copper grain size and distribution, where grain boundary diffusion is found to be a dominant failure mechanism. *Published by AIP Publishing.* [http://dx.doi.org/10.1063/1.4947582]

I. INTRODUCTION

Electromigration (EM) is a large concern for the reliability of electronic on-chip interconnects. The continuous decrease in dimensions is detrimental to EM lifetimes of Cu interconnects because of the increasing current densities, decreased critical void volume, and the use of low-k dielectrics.[1,2] Soon the half-pitch of local interconnects will reach values below 10 nm and at this point copper will need to be replaced by other materials because of the strong increase in resistivity[3] and deterioration of electromigration performance.[4] Alternative interconnect materials have been proposed[5,6] and are currently in research. Testing the EM properties of these materials is of key importance. Moreover, at these very narrow dimensions, different physical mechanisms play a role in EM failure and understanding them is essential for a good material choice and design of the interconnect.

There is an urgent need for a fast test method to assess the EM performance of different materials and to provide reliable insights into the underlying physical mechanisms of electromigration. The present, widely used test method already dates from the 1960s. In this test method a large number of samples are stressed at various elevated temperatures and current densities until failure occurs. Subsequently, extrapolations are made to obtain lifetimes at normal operation conditions using Black's law.[7] This test method has some important drawbacks: it is time-consuming (test times are several weeks to months), destructive, and is limited in providing physical understanding of EM. Furthermore, the high stress conditions lead to different failure mechanisms than under normal operation,[8] which causes test-times of hundreds of hours. Some authors argue that this test method cannot unambiguously determine EM lifetimes and activation energies.[9]

As a solution, the use of 1/f noise measurements for faster evaluation of electromigration is proposed. This technique was already introduced for damage detection in aluminum thin films and interconnects[10–12] and later also for EM assessment,[13–22] but was never used to study copper or other interconnect materials. Moreover, as line widths of leading edge interconnects are in the range of 20–30 nm, we believe that 1/f noise measurements are more sensitive to the presence of defects and the activation of physical mechanisms than in the past, when line widths were in the micrometer range.

In this paper it is shown that 1/f noise measurements can indeed be used for EM characterization and provide more fundamental understanding of EM mechanisms in advanced interconnects. The applications of 1/f noise investigated in this paper are: (a) whether they can serve as an early indicator for EM damage, (b) whether a qualitative relation exists between defect concentrations and EM lifetimes, and (c) whether a correlation exists between the activation energies obtained from 1/f spectra and activation energies obtained from classic EM-tests.

Additionally, the 1/f noise measurements are used to assess and compare the electromigration characteristics of various interconnect materials. The results are shown for two types of damascene copper, direct etched copper[23] and tungsten lines.

[a)]sofie.beyne@imec.be

II. EXPERIMENTAL PROCEDURE

A. Noise measurements

Noise measurements are carried out at wafer level using the commercial Berkeley Technology Associates (BTA) setup (see Figure 1) with ProPlussolutions software. The measurements are performed with a constant current and the noise Power Spectral Density (PSD) is derived based on the registered resistance fluctuations in the frequency band 2 Hz–100 kHz. To compare different samples, the PSD is evaluated at 5 Hz and each PSD value is normalized by dividing by the current squared. The PSD provides information on how the power is distributed in the frequency domain. 1/f noise is a type of noise where the PSD is proportional to $1/f^m$, with m typically close to 1, but where m can also take values >2, in which case it is referred to as $1/f^2$ noise.

For the first application of 1/f noise, where it is proposed as an early indicator of EM damage, a wafer level EM stress test is combined with noise measurements. The sample is stressed with a high current density (84 MA/cm^2) and at an elevated temperature (200 °C). After certain stress times, a much smaller sense current (3 MA/cm^2) is applied to measure the current fluctuations in the interconnect during 4 s. Based on these current fluctuations (denoted by $i(t)$, where t stands for time (s)) the frequency domain signal ($I(f)$) is calculated with the Fourier transformation (j is used to denote the imaginary unit $\sqrt{-1}$)

$$I(f) = \int_{-\infty}^{+\infty} i(t)\exp(-j2\pi ft)dt, \tag{1}$$

and the Power Spectral Density (PSD), also denoted as S_{xx}, is calculated as:

$$PSD = S_{xx}(f) = \lim_{P\to\infty}\frac{1}{P}|I_P(f)|^2, \tag{2}$$

where P is the period of the periodic signal and I_P the Fourier transform of the signal $i_P(t)$ which is the signal $i(t)$ over a period $[-P/2, P/2]$. After performing this non-destructive noise measurement, the device is stressed again at higher current density (84 MA/cm^2). This procedure is repeated until failure occurs, defined as a 20% change in resistance.

In the second application, 1/f noise is applied to qualitatively compare the EM lifetime by measuring the current dependence of the 1/f noise at a fixed temperature. The current ranges from 10^{-6} A to 10^{-3} A. This corresponds to a current density of 0.03 MA/cm^2 and 30 MA/cm^2 in the interconnects

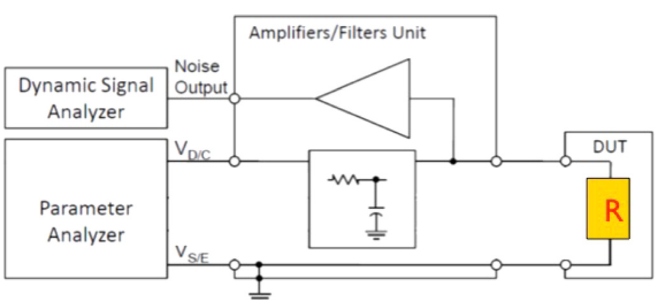

FIG. 1. Noise measurement setup (Berkeley Technology Associates).

with 30 nm line width and slightly lower values in the lines of ≈40 nm width. The temperature is kept constant at 125 °C. The PSD of the noise (evaluated at 10 Hz) is plotted as a function of current.

For the third application of 1/f noise, in which activation energies are studied, the temperature dependence of the noise is measured at a fixed current, 50 μA or 100 μA (1.5 and 3 MA/cm^2, respectively) and at temperatures in the range of 25 °C–200 °C (this range is determined by the constraints of the measurement system). Under these conditions electromigration is assumed not to occur. The PSD of the noise (evaluated at 5 Hz) is plotted as a function of temperature. The temperature dependence of 1/f noise in thin films has extensively been discussed in the literature.[24–30] The model of Dutta, Dimon, and Horn is the most generally accepted. That so-called "DDH model" can be used to calculate the distribution of activation energies $D(E_a)$ based on the temperature dependence of the noise PSD, denoted as $S(\omega, T)$.

The activation energy $\tilde{E_a}$ at which the distribution function $D(\tilde{E_a})$ peaks is given by the following equation:[27]

$$\tilde{E_a} \equiv -k_B T \ln(\omega\tau_0), \tag{3}$$

where k_B is the Boltzmann constant 8.617343×10^{-5} eV/K, T is the temperature (in Kelvin), ω is the angular frequency ($\omega = 2\pi f$), and τ_0 is the inverse attempt frequency f_0, hereafter defined as 10^{-13}. Note that this factor τ_0 does not differ too much between the different materials that are tested and a small variation in its value only has a minor influence on $\tilde{E_a}$.

To calculate the distribution function $D(\tilde{E_a})$, the DDH model requires three explicit assumptions:[27] (1) the 1/f noise is caused by a superposition of random fluctuations with thermally activated characteristic times; (2) the distribution of activation energies $D(\tilde{E_a})$ must be "smooth," in a sense that it varies slowly over $\Delta E_a \approx k_B T$; and (3) the "attempt frequency" $f_0 = 1/\tau_0 \gg f$, with f the frequency at which the noise is measured. Taking into account the previous assumptions, the following formula is derived to calculate the distribution of activation energies $D(\tilde{E_a})$:

$$D\left(\tilde{E_a}\right) \propto \frac{\omega}{k_B T} S(\omega, T), \tag{4}$$

where $\tilde{E_a}$ is again the activation energy at which the distribution function D peaks and $S(\omega, T)$ is the normalized PSD as a function of frequency and temperature. Using the above Equations (3) and (4), a distribution of activation energies is calculated and activation energies can be determined based on the maxima of the function $D(E)$.

B. Standard EM tests

Also standard EM tests are carried out on packaged samples (with classical 4-point structures) under accelerated test conditions (for Cu samples current densities of 1–5 MA/cm^2 and temperatures of 250–350 °C are used). Failure is defined as the moment that a 20% change in resistance occurs. Black's law[7] is then applied to extrapolate the EM lifetimes to normal operation conditions and to calculate EM activation energies.

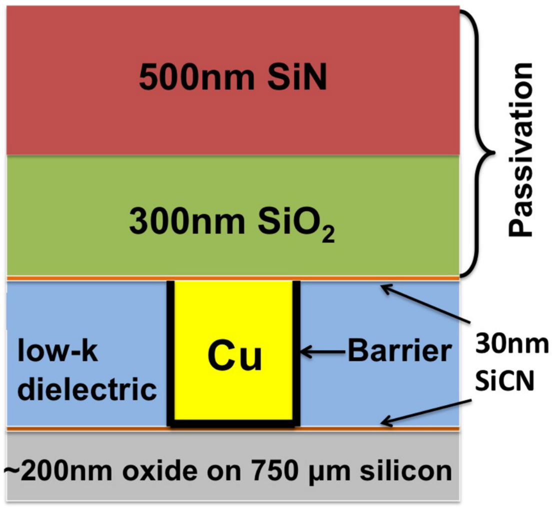

FIG. 2. Schematic cross section of the single damascene Cu lines. In these experiments the barrier was either 3 nm TaNTa or 3 nm RuTiN.

C. Sample description

In this paper, 4 samples are considered:

- Two types of damascene copper lines (a schematic cross section of the Cu damascene samples is shown in Figure 2). The two types of damascene copper differ from each other by their barrier layer, which is either 3 nm TaNTa or 3 nm RuTiN.
- Copper lines integrated using Cu direct etch. It is important to note that the direct etched Cu is not damascene and has larger, columnar grains. The resistivity of these samples was lower than that for damascene copper of similar dimensions because of the reduced grain boundary scattering.[23]
- Tungsten. This sample is barrier-less and strongly polycrystalline, with some key-hole voids present as can be seen in the cross section in Table I.

The properties of the various samples and EM activation energies obtained with both classic tests and 1/f noise measurements are shown in Table I. The deduction of these 1/f noise activation energies will be explained in Section III C. In what follows, we refer to the samples using the short description given in Table I. The low EM activation energy for the *TaNTa* sample might be surprising, but it was obtained using local sense structures to measure the first onset to failure.[31] The sample *RuTiN* is not currently used in industry because the RuTiN barrier is not scalable below 3 nm, but it has been included nonetheless in order to have a more extensive comparison of different samples.

III. RESULTS AND DISCUSSION

In this section the results of the different applications of 1/f noise measurements are shown and discussed.

A. 1/f noise measurements as an early indicator for EM damage

In this experiment the sample *TaNTa* (see Table I) was submitted to an EM stress test combined with noise measurements. Figure 3(a) shows the relative resistance changes during the experiment. The PSD of the noise after different stress times, 4, 66, and 90 s, is shown in Figure 3(b). Failure occurs after a stress time of about 120 s, as indicated by the sudden increase in resistance in Figure 3(a). There is no indication in this graph of damage prior to failure. However, in Figure 3(b), it can be seen that the PSD of the noise increased by several orders of magnitude before changes in the resistance were observed. These results are in line with measurements on aluminum-samples.[15,16,22] In our experiments, also the frequency exponent of the noise PSD gives useful information. For example, in Figure 3(b), it can be seen that the frequency exponent changed from 1 to 2 after 66 s of stress. Some authors[16,17,32] have correlated frequency exponents larger than 2 with EM atom fluxes, void formation, and irreversible damage. Void formation is indeed plausible considering that to have a frequency exponent of 2, the underlying time-domain signal must exhibit a step-like behavior, as is indeed the case for a void causing a jump in current flow. However, evidence of the irreversible nature of those defects is lacking as it is probable that some defects have formed only temporarily and disappear again after a certain amount of time. When the interconnect line width

TABLE I. Specifications of the test samples.

Name	Grain structure	Cross section	Barrier	Line width (nm)	EM E_A (eV)	1/f E_A (eV)
Cu direct etch	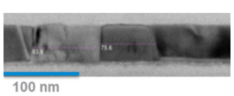	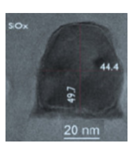	Bottom: Ta, sidewall and top: SiCN	45	1.10	≤0.70 and ≥1.10
TaNTa (damasceen)	Polycrystalline	see Figure 2	3 nm TaNTa	30	0.74	0.76–0.78
RuTiN (damasceen)	Polycrystalline	see Figure 2	3 nm RuTiN	30	0.79	0.79–0.81 and ≥ 1.10
W	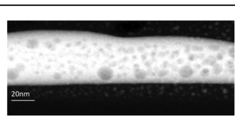	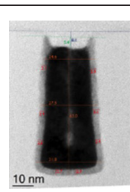	/	37	0.69	0.73–0.75

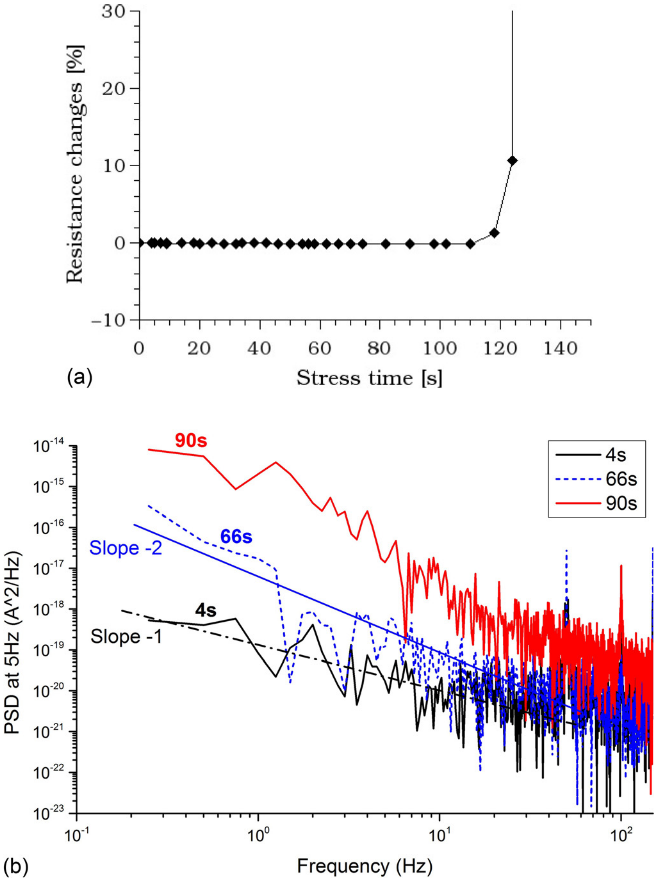

FIG. 3. (a) The changes in resistance during the EM stress test. (b) The evolution of the PSD after different EM stress times.

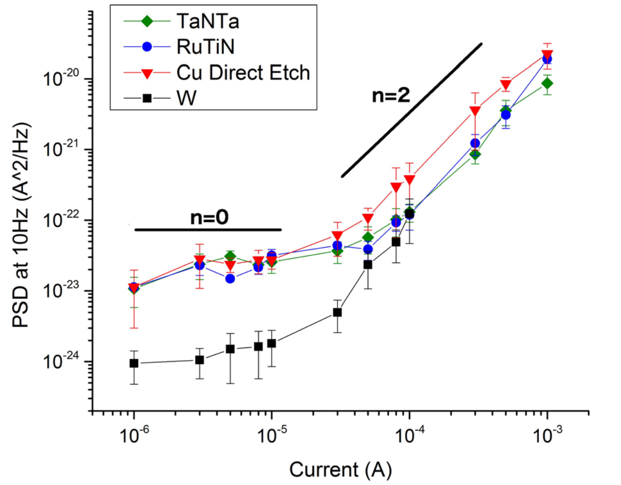

FIG. 4. The noise PSD, evaluated at 10 Hz, as a function of current for the different interconnect types (see Table I).

was much larger, around 1 μm, the early initiation of a void had only a minor influence on the current fluctuations in the conductor and was probably not observable.[16,17] Only a void that has already grown to a considerable size as compared with the line thickness will indeed be detected by 1/f noise measurements. In this respect, the hypothesis of linking the occurrence of frequency exponents larger than 2 to irreversible damage is indeed plausible. In our case, however, the line width of the interconnects is so small, $\approx$30 nm, that also the initiation of voids is likely to be visible in the 1/f noise measurements, but it is not *a-priori* known if that void will also propagate and eventually cause irreversible EM damage. To summarize, it is believed that the change in frequency exponent, observed in Figure 3(b), is related to the formation of voids, as also confirmed by the literature,[29,33] but its irreversible nature remains ambiguous. Nevertheless, together with the increasing magnitude of the noise PSD, frequency exponents larger than 2 do indicate that EM failure is imminent, as can be seen in Figure 3(b).

B. Current dependence of 1/f noise

In this experiment the current dependence of 1/f noise in the different interconnect types is investigated. More information on the experimental setup can be found in Section II A. The results are shown in Figure 4. In the current range 10^{-6} A–10^{-3} A the curves generally consist of two stages. They can be described by a power law relationship $PSD \propto I^n$ in which n is 0 for the first and about 2 for the second stage. Up till now, only the second stage, where n = 2, has been described in the literature,[34] but only empirically. The part of the curve where $n = 0$ is valuable when comparing the noise magnitude of different materials. This stems from the fact that it would be better to consider current density instead of current. Current is an extensive parameter which is meaningless when comparing materials with different cross sections. Unfortunately, the cross sections of the different samples are not precisely known (and variations in cross section on a wafer are not unlikely). The current density, however, no longer depends on the dimensions of the samples and allows a more precise comparison. When the $PSD \propto I^0$, a small shift to left or right of the curve (when the cross sections differ) will not result in a change in PSD, which makes a comparison much more reliable.

With Figure 4, the PSD values of the different samples are compared in the current range 10^{-6} A–10^{-5} A. The frequency at which the PSD is evaluated will influence the location of the graphs. Since the effect of defects on the noise PSD is visible in the frequency band 0 to 10 Hz,[32] and higher frequencies correspond to faster mechanisms, the PSDs of the different materials are compared at 10 Hz. No significant difference in noise PSD between the different types of Cu can be observed. Nevertheless, tungsten, which has a very long EM lifetime, has significantly lower noise in the current range 10^{-6}–10^{-4} A. In Section III A, it was demonstrated that 1/f noise can be used as an early damage indicator since its magnitude is very sensitive to the presence of defects. Also electromigration is greatly influenced by defects: a sample with a higher defect concentration will have significantly lower EM lifetimes than a sample with low defect concentration.[21] This implies that the noise level of a material could be an indication of its EM lifetime. This hypothesis is indeed confirmed by the low noise PSD and high EM lifetime of tungsten as compared to copper.

The question arises whether the differences in noise between samples of the same material are an indication of the amount of defects and consequently also the EM lifetime t_{50}. To investigate this, the current dependence of the noise PSD of several *TaNTa* samples was measured. Their position on

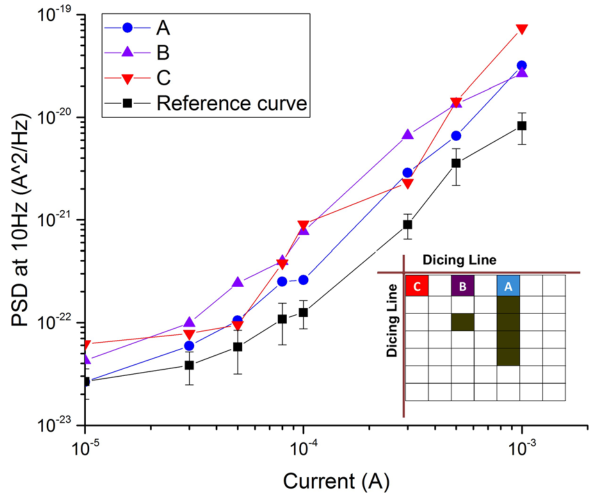

FIG. 5. The noise PSD (at 10 Hz), as a function of current for various *TaNTa* samples. The position of the samples on the wafer piece is illustrated in the bottom right corner. The average noise PSD is based on the dies in the center. The dies close to the dicing line (A, B, and C) clearly exhibit noise that is above average.

the wafer varied in such a way that some samples were close to the dicing edge such that they were no longer contained by a dicing ring, which inhibits the absorption of moisture. Besides moisture intake, we suggest that also stress change or propagation of micro-cracks might contribute to a higher defect concentration in the samples close to the dicing edge (A, B, and especially C in Figure 5). Therefore, we propose that the samples close to the edge are likely to exhibit a higher noise level and possibly a lower EM lifetime. This is indeed confirmed by Figure 5 where the noise of the dies is shown as well as their position on the wafer. The samples close to the dicing line have PSD values clearly above average.

C. Temperature dependence of 1/f noise

In this section we investigate the correlation between activation energies observed through measurements of the temperature dependence of 1/f noise and those obtained during classic EM tests. The methodology is shown for the *TaNTa sample* (see Table I) in Figure 6, where the

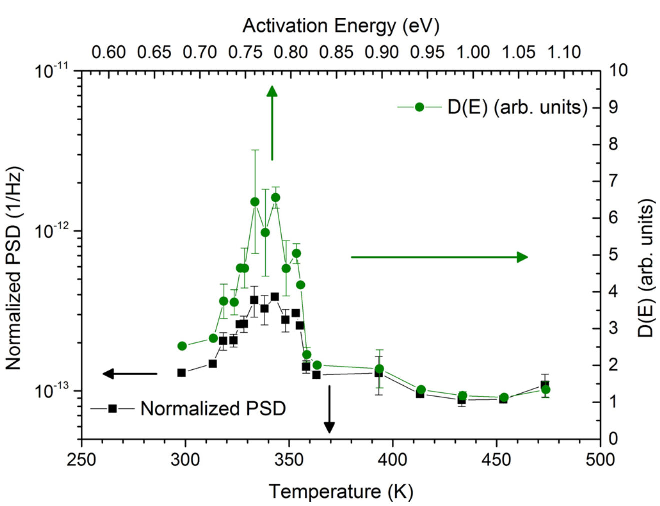

FIG. 6. Based on the temperature dependence of the noise (black squares), the distribution of activation energies (green dots) is calculated.

temperature dependence of the noise PSD is indicated by the black squares. Then, a distribution of activation energies is calculated, based on Equation (4). The distribution function $D(E_a)$ as a function of the activation energy E_a is indicated by the green dots in Figure 6. From that graph, the activation energy can be calculated based on the maxima of the

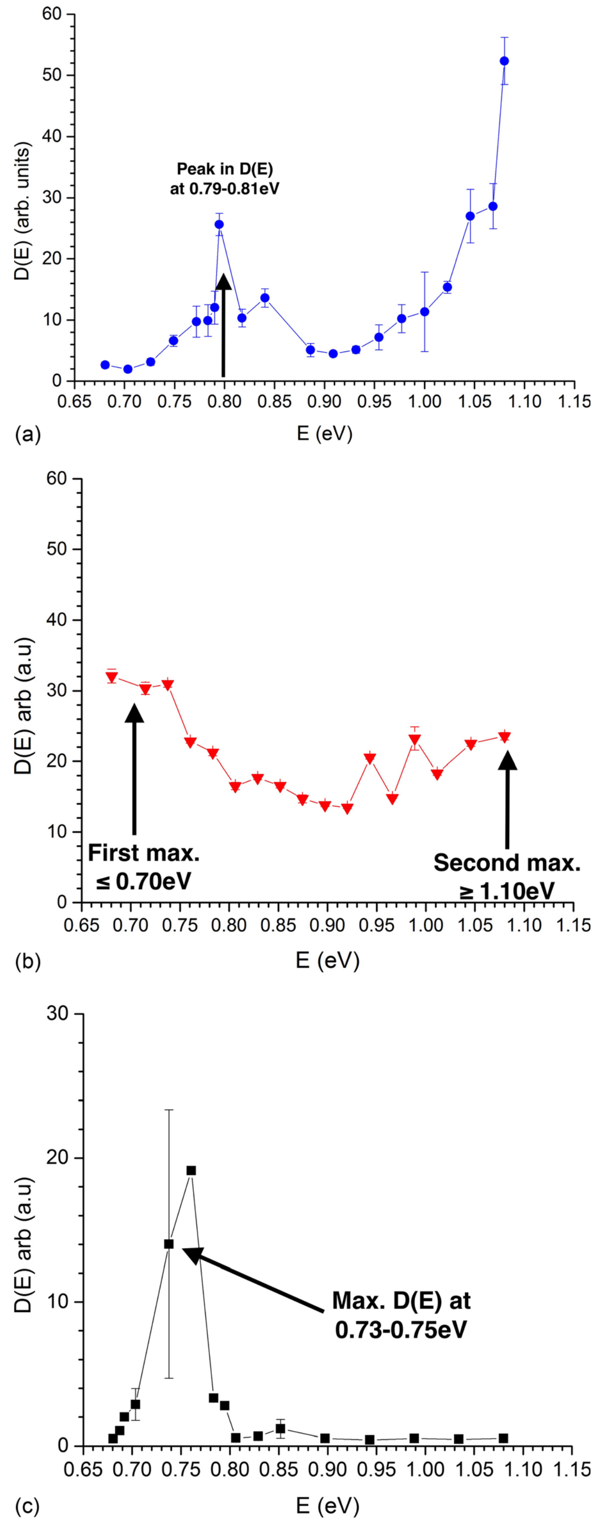

FIG. 7. The *RuTiN sample* (a) shows a peak in D(E) at 0.79–0.81 eV and a second increase in D(E) above 1 eV. The *Cu Direct etch sample* (b) shows 2 maxima in D(E), the first one $\leq$ 0.7 eV and the second one $\geq$ 1.1 eV. The *W sample* (c) shows a peak in D(E) at 0.73–0.75 eV.

function $D(E_a)$. In Figure 6, a maximum at 0.76–0.78 eV is found. This corresponds to the physical mechanisms that become activated at 330–340 K (60–70 °C). This methodology was repeated for the other samples in Table I. Figures 7(a)–7(c) show the distribution of activation energies for the samples *RuTiN*, *Cu Direct Etch,* and *W,* respectively. The activation energies are again determined based on the maxima of the function $D(E_a)$ and are summarized in the last column of Table I. Figure 8 shows the calculated distribution of activation energies for all the samples. All the samples in Table I are polycrystalline, except for Cu direct etch (see also its grain structure in Table I). All these polycrystalline samples show a maximum in $D(E_a)$ around 0.75–0.80 eV. When comparing the last two columns of Table I, it is clear that the 1/f noise activation energies correspond to a great extent to the values for electromigration obtained using the classic accelerated tests. This suggests that the mechanisms responsible for the thermally activated increases in noise PSD, also act as the dominant EM diffusion mechanisms. It is believed that the typical activation energies of 0.75–0.80 eV, which are observed in all the polycrystalline samples, are related to grain boundary diffusion. Electromigration in copper lines has long been believed to be dominated by diffusion at the copper–dielectric cap interface, but as the line widths decrease and the samples become increasingly polycrystalline, grain boundary diffusion has been suggested as the dominant EM failure mechanism.[35–38] This is also confirmed by the activation energies found with the 1/f noise measurements. The values also correspond well to the activation energies typically linked to grain boundary diffusion in Cu.[39,40]

Since the location of the maximal noise PSD around 0.8 eV is similar for the Cu samples with TaNTa and RuTiN barrier, the activation energy linked to that peak is not likely to be related to the Cu–barrier interface. Also, Cu-dielectric surface diffusion is less likely to be related to the 0.8 eV peak, since without doping (as in this case), values for Cu-dielectric surface diffusion have been reported to be in the range of 0.95 eV.[36] Only, for the Cu sample with RuTiN barrier, a significant increase in $D(E_a)$ at higher activation energies can be seen, which might be an indication of a weak Cu-dielectric interface.

Figure 9 shows the frequency exponent as a function of temperature. This graph allows us to see at which temperature the maximal frequency exponent is reached. All the polycrystalline samples behave similarly in the temperature range 55–100 °C (corresponding to activation energies of 0.75–0.85 eV): the frequency exponent increases similarly as the magnitude of the PSD, reaching values close to or above 2. This implies that the mechanism that becomes activated at that point is of a different nature than the ones leading to generic 1/f noise. The sample *RuTiN* shows a continuous increase in frequency exponent above 100 °C. The sample *Cu Direct Etch* behaves differently; the frequency exponent stays within the range of generic 1/f noise ($0.7 \leq m \leq 1.4$), so the physical mechanism is believed to be different. This enforces the hypothesis that activation energies close to 0.80 eV can be linked to grain boundary diffusion. The activation energy of 1.1 eV in Cu Direct Etch (which has columnar grains) is more likely to be related to interface properties.

In Figure 7(c) the distribution of activation energies is shown for W. The maximum in $D(E)$ indicates an activation energy of 0.73–0.75 eV. Table I shows that this value is in line with the low EM activation energy of 0.69 eV that was obtained with classic tests. Nevertheless, the two values differ slightly. It should be noted that it was very difficult to obtain the EM activation energy for W with the classic test method because of its very long EM lifetime. Moreover, the activation energy obtained with the accelerated test might also be dependent on the current density that was used during

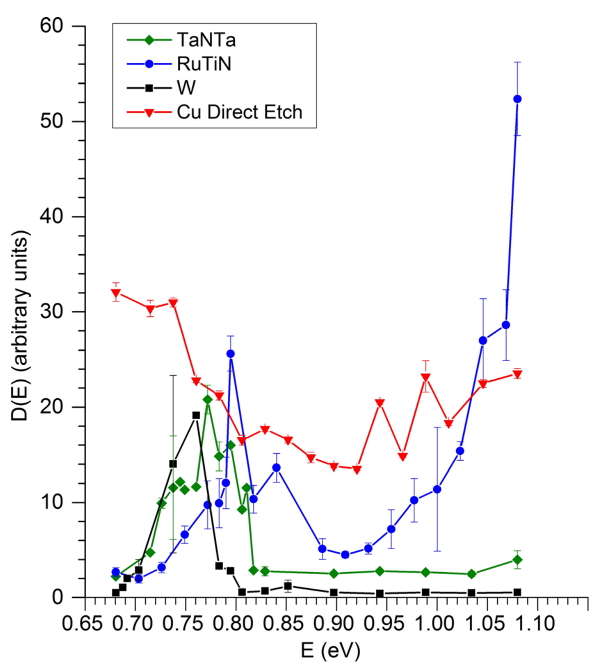

FIG. 8. Distribution of activation energies for the samples in Table I, calculated based on the temperature dependence of the noise PSD with formula 4.

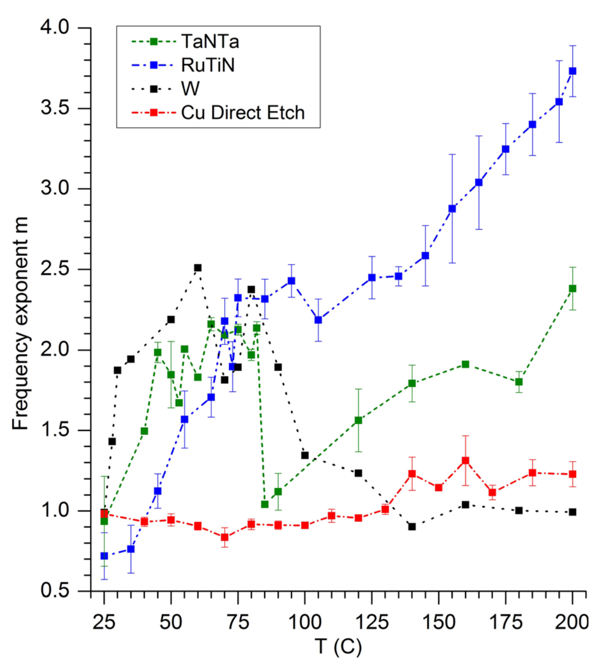

FIG. 9. Frequency exponent as a function of temperature in °C.

the test,[9] or give a value that is actually more of an average of different mechanisms rather than one specific.

One could argue that the activation energy of tungsten around 0.70–0.75 eV is too low to be related to grain boundary diffusion. The vacancy formation energy for W in the lattice is 3.6 eV (Ref. 41) and the vacancy migration energy 1.7 eV,[41] giving a self-diffusion activation energy of 5.3 eV. Nevertheless, one should keep in mind that the activation energies for grain boundary diffusion are much lower than those for self-diffusion, as the grain boundary already contains many defects.[42] Finding literature data about the activation energy for grain boundary diffusion in tungsten that is also applicable to these specific samples is difficult: the temperature history of the material as well as the grain size influence the activation energy.[43] To our current knowledge no studies have been performed about grain boundary diffusion in tungsten comparable with our samples. Yet, an analysis of the possible point defects in tungsten has shown that there are several vacancy-related activation energies in the range of 0.70 eV: a vacancy relaxation energy of 0.75 eV (Ref. 44) (the atoms surrounding the vacancy exhibit relaxation by a co-operative motion) and a second nearest neighbor divacancy binding energy of 0.70 eV (Ref. 45) or 0.78 eV (Ref. 44) (depending on the source). Given the fact that many vacancies were already present in the tungsten lines prior to EM stress, it is not unlikely that mechanisms similar to these play a role in the diffusion mechanism observed by 1/f noise measurements in the range of 0.73–0.75 eV and consequently also in electromigration failure.

A point of discussion that could arise for the above calculations of activation energies is the correct application of the DDH model in Eq. (4). Indeed, the three aforementioned assumptions of this model must still be valid. The first and third assumptions are indeed reasonable, but for the second assumption, namely, that the distribution of activation energies $D(\tilde{E}_a)$ must vary slowly over $\Delta E_a \approx k_B T$, discussion may arise because the peak in, for example, Figure 6 is rather sharp. This approximation originates from a simplification of the original equation proposed by Dutta and Horn,[28] where only the first term of a Taylor series expansion of D(E) was considered. When modifying their approach by allowing the possibility of $D(\tilde{E}_a)$ being a fourth order function of E_a, the assumption of $D(\tilde{E}_a)$ varying slowly over $\Delta E_a \approx k_B T$ would no longer be necessary. Nevertheless, the classic DDH model has always been used successfully in literature. Yet, it seems appropriate to explore this adaptation of the DDH model. The mathematical derivation as well as the introduction of new boundary conditions (a consequence of the fourth order term) are out of the scope of this paper, and will be explored in future work.

IV. CONCLUSIONS

As classic electromigration test methods are destructive, time consuming, and provide only limited information about the physical mechanisms, we explored the use of 1/f noise measurements as a technique for electromigration characterization. Where the applicability of this method was already studied, with limited success, for aluminum-based interconnects, we demonstrated its potential for copper wires with line widths in the nanometer range and for alternative metals currently considered by the industry as a replacement for copper in future interconnects. Three different types of noise measurements were explored, each leading to useful information on the electromigration performance of our materials:

- Monitoring 1/f noise during electromigration stress tests provides an early indication of EM damage, i.e., before changes in the resistance can be observed.
- Curves of the 1/f noise PSD as a function of current can be used to make a qualitative comparison of interconnects in terms of the amount of defects and their electromigration lifetime. This could enable damage detection already in early production steps or during operation.
- From the temperature dependence of the 1/f noise PSD, activation energies can be calculated. These show great similarities with activation energies obtained from classic electromigration tests. A link between the mechanisms responsible for thermally activated increases in 1/f noise and EM failure mechanisms can be established, which makes this type of measurements useful to obtain insights in electromigration mechanisms.

ACKNOWLEDGMENTS

The authors would like to thank all imec colleagues and professors from the department of materials engineering at KU Leuven that contributed to this work and, in particular, the AMSIMEC staff members. The authors also thank the fund for scientific research in Flanders, FWO (Fonds voor Wetenschappelijk Onderzoek) who funded this research.

[1]P. S. Ho, K.-D. Lee, S. Yoon, X. Lu, and E. T. Ogawa, Mater. Sci. Semicond. Process. **7**, 157 (2004).
[2]K. Croes, K. Moon, L. Carbonell, H. Struyf, N. Heylen, Z. Tőkei, and G. Beyer, in *Proceedings of the Advanced Metallization Conference* (2007), Vol. 2008, pp. 711–715.
[3]P. Kapur, J. McVittie, and K. Saraswat, IEEE Trans. Electron Devices **49**, 590 (2002).
[4]C.-K. Hu, R. Rosenberg, H. Rathore, D. Nguyen, and B. Agarwala, in *IEEE International Conference on Interconnect Technology* (IEEE, 1999), pp. 267–269.
[5]K. Sankaran, S. Clima, M. Mees, C. Adelmann, Z. Tőkei, and G. Pourtois, in *IEEE International Interconnect Technology Conference/Advanced Metallization Conference (IITC/AMC)* (IEEE, 2014), pp. 193–196.
[6]C. Adelmann, L. Wen, A. Peter, Y. Siew, K. Croes, J. Swerts, M. Popovici, K. Sankaran, G. Pourtois, S. Van Elshocht *et al.*, in *IEEE International Interconnect Technology Conference/Advanced Metallization Conference (IITC/AMC)* (IEEE, 2014), pp. 173–176.
[7]J. Black, in *Sixth Annual Reliability Physics Symposium* (IEEE, 1967), pp. 148–159.
[8]J. Lloyd, Microelectron. Reliab. **47**, 1468 (2007).
[9]M. Hauschildt, C. Hennesthal, G. Talut, O. Aubel, M. Gall, K. Yeap, and E. Zschech, in *IEEE International Reliability Physics Symposium (IRPS)* (IEEE, 2013), pp. 2C–1.
[10]J. Vossen, Appl. Phys. Lett. **23**, 287 (1973).
[11]J. Pelz and J. Clarke, Phys. Rev. Lett. **55**, 738 (1985).
[12]J. Cottle and N. Klonaris, J. Electron. Mater. **19**, 1201 (1990).
[13]M. Van den Homberg, A. Verbruggen, P. Alkemade, S. Radelaar, E. Ochs, K. Armbruster-Dagge, A. Seeger, and H. Stoll, Phys. Rev. B **57**, 53 (1998).
[14]A. Diligenti, B. Neri, P. Bagnoli, A. Barsanti, and M. Rizzo, IEEE Electron Device Lett. **6**, 606 (1985).
[15]R. Koch, J. Lloyd, and J. Cronin, Phys. Rev. Lett. **55**, 2487 (1985).

[16]T. Chen, T. Djeu, and R. Moore, in *23rd Annual Reliability Physics Symposium* (IEEE, 1985), pp. 87–92.
[17]B. Neri, A. Diligenti, and P. Bagnoli, IEEE Trans. Electron Devices **34**, 2317 (1987).
[18]J. Cottle, "Excess noise and its relationship to electromigration in thin film interconnections," Ph.D. thesis, University of South Florida, 1987.
[19]J. Cottle, T. Chen, and K. Rodbell, in *26th Annual International Reliability Physics Symposium* (IEEE, 1988), pp. 203–208.
[20]A. Diligenti, P. Bagnoli, B. Neri, S. Bea, and L. Mantellassi, Solid-State Electron. **32**, 11 (1989).
[21]T. Chen and A. Yassine, IEEE Trans. Electron Devices **41**, 2165 (1994).
[22]K. Dagge, W. Frank, A. Seeger, and H. Stoll, Appl. Phys. Lett. **68**, 1198 (1996).
[23]L. Wen, F. Yamashita, B. Tang, K. Croes, S. Tahara, T. Maeshiro, E. Nishimura, F. Lazzarino, I. Ciofi, J. Boemmels, and Z. Tőkei, in IEEE International Interconnect Technology Conference (IITC) (2015).
[24]R. Voss and J. Clarke, Phys. Rev. Lett. **36**, 42 (1976).
[25]J. W. Eberhard and P. M. Horn, Phys. Rev. Lett. **39**, 643 (1977).
[26]D. Fleetwood, D. Beutler, J. Masden, and N. Giordano, J. Appl. Phys. **61**, 5308 (1987).
[27]P. Dutta, P. Dimon, and P. Horn, Phys. Rev. Lett. **43**, 646 (1979).
[28]P. Dutta and P. Horn, Rev. Mod. Phys. **53**, 497 (1981).
[29]M. Celasco, F. Fiorillo, and P. Mazzetti, Phys. Rev. Lett. **36**, 38 (1976).
[30]M. Weissman, Rev. Mod. Phys. **60**, 537 (1988).
[31]T. Kirimura, K. Croes, Y. Siew, K. Vanstreels, P. Czarnecki, Z. Ei-Mekki, M. Van Der Veen, D. Dictus, A. Yoon, A. Kolics *et al.*, in *IEEE International Interconnect Technology Conference (IITC)* (IEEE, 2013), pp. 1–3.
[32]E. Simoen and C. Claeys, Semicond. Sci. Technol. **14**, R61 (1999).
[33]G. P. Zhigal'skii, Phys.-Usp. **40**, 599 (1997).
[34]F. Hooge, T. Kleinpenning, and L. Vandamme, Rep. Prog. Phys. **44**, 479 (1981).
[35]C.-K. Hu, J. Ohm, L. Gignac, C. Breslin, S. Mittal, G. Bonilla, D. Edelstein, R. Rosenberg, S. Choi, J. An *et al.*, J. Appl. Phys. **111**, 093722 (2012).
[36]M. Lin, S. Lee, and A. Oates, in *IEEE International Reliability Physics Symposium (IRPS)* (IEEE, 2010), pp. 705–711.
[37]A. Oates and M. Lin, in *IEEE International Reliability Physics Symposium (IRPS)* (IEEE, 2012), pp. 6B–2.
[38]A. S. Oates, ECS J. Solid State Sci. Technol. **4**, N3168 (2015).
[39]M. R. Sørensen, Y. Mishin, and A. F. Voter, Phys. Rev. B **62**, 3658 (2000).
[40]L. Arnaud, T. Berger, and G. Reimbold, J. Appl. Phys. **93**, 192 (2003).
[41]P. Ehrhart, P. Jung, H. Schultz, and H. Ullmaier, *Atomic Defects in Metals/Atomare Fehlstellen in Metallen* (Springer, 1991), Vol. 25.
[42]D. Gupta, *Diffusion Processes in Advanced Technological Materials* (Springer Science & Business Media, 2010).
[43]R. Würschum, S. Herth, and U. Brossmann, Adv. Eng. Mater. **5**, 365 (2003).
[44]R. A. Johnson, Phys. Rev. B **27**, 2014 (1983).
[45]J. Y. Park, H. C. W. Huang, R. W. Siegel, and R. W. Balluffi, Philos. Mag. A **48**, 397 (1983).